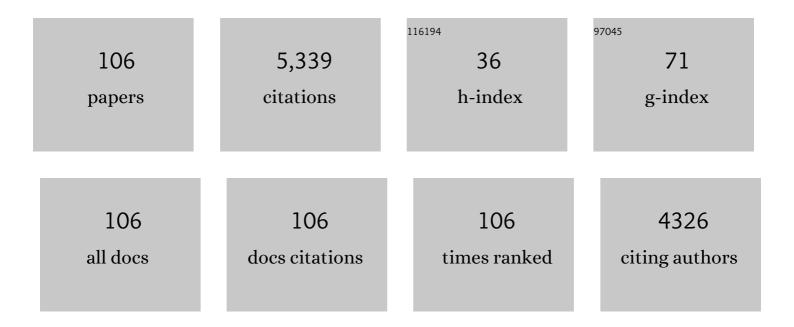
## Xiaohong Zhang

List of Publications by Year in descending order

Source: https://exaly.com/author-pdf/3718634/publications.pdf Version: 2024-02-01



Хилономс 7нлыс

#	Article	IF	CITATIONS
1	Global Ionospheric Modeling Using Multi-GNSS and Upcoming LEO Constellations: Two Methods and Comparison. IEEE Transactions on Geoscience and Remote Sensing, 2022, 60, 1-15.	2.7	19
2	An enhanced foot-mounted PDR method with adaptive ZUPT and multi-sensors fusion for seamless pedestrian navigation. GPS Solutions, 2022, 26, 1.	2.2	12
3	Frequency design of LEO-based navigation augmentation signals for dual-band ionospheric-free ambiguity resolution. GPS Solutions, 2022, 26, 1.	2.2	5
4	Investigating GNSS PPPâ $\in$ "RTK with external ionospheric constraints. Satellite Navigation, 2022, 3, .	4.6	22
5	Study on the Relationship Between the Equivalent GDOP and the Convergence Time of LEO-Augmented BDS PPP. Lecture Notes in Electrical Engineering, 2022, , 244-254.	0.3	1
6	Assessment of the performance of GPS/Galileo PPP-RTK convergence using ionospheric corrections from networks with different scales. Earth, Planets and Space, 2022, 74, .	0.9	7
7	Investigation on Horizontal and Vertical Traveling Ionospheric Disturbances Propagation in Globalâ€6cale Using GNSS and Multiâ€LEO Satellites. Space Weather, 2022, 20, .	1.3	5
8	PPP-RTK considering the ionosphere uncertainty with cross-validation. Satellite Navigation, 2022, 3, .	4.6	15
9	The Performance of Three-Frequency GPS PPP-RTK with Partial Ambiguity Resolution. Atmosphere, 2022, 13, 1014.	1.0	4
10	Evaluation and validation of various rapid GNSS global ionospheric maps over one solar cycle. Advances in Space Research, 2022, 70, 2494-2505.	1.2	4
11	lonospheric Total Electron Content Estimation Using GNSS Carrier Phase Observations Based on Zero-Difference Integer Ambiguity: Methodology and Assessment. IEEE Transactions on Geoscience and Remote Sensing, 2021, 59, 817-830.	2.7	32
12	Analysis of Atmospheric and Ionospheric Variations Due to Impacts of Super Typhoon Mangkhut (1822) in the Northwest Pacific Ocean. Remote Sensing, 2021, 13, 661.	1.8	19
13	Common-mode error and multipath mitigation for subdaily crustal deformation monitoringÂwithÂhigh-rateÂGPS observations. GPS Solutions, 2021, 25, 1.	2.2	10
14	Single-epoch RTK performance assessment of tightly combined BDS-2 and newly complete BDS-3. Satellite Navigation, 2021, 2, .	4.6	18
15	Estimation and analysis of multi-GNSS observable-specific code biases. GPS Solutions, 2021, 25, 1.	2.2	14
16	LEO Constellation-Augmented Multi-GNSS for 3D Water Vapor Tomography. Remote Sensing, 2021, 13, 3056.	1.8	7
17	Precise Orbit Determination for LEO Satellites With Ambiguity Resolution: Improvement and Comparison. Journal of Geophysical Research: Solid Earth, 2021, 126, e2021JB022491.	1.4	11
18	Electron Density Reconstruction by Ionospheric Tomography From the Combination of GNSS and Upcoming LEO Constellations. Journal of Geophysical Research: Space Physics, 2021, 126, e2020JA029074.	0.8	10

#	Article	IF	CITATIONS
19	Multi-GNSS contributions to differential code biases determination and regional ionospheric modeling in China. Advances in Space Research, 2020, 65, 221-234.	1.2	16
20	Multi-GNSS fractional cycle bias products generation for GNSS ambiguity-fixed PPP at Wuhan University. GPS Solutions, 2020, 24, 1.	2.2	38
21	Topside Ionosphere of NeQuick2 and IRIâ€2016 Validated by Using Onboard GPS Observations From Multiple LEO Satellites. Journal of Geophysical Research: Space Physics, 2020, 125, e2020JA027999.	0.8	10
22	Mapping topside ionospheric vertical electron content from multiple LEO satellites at different orbital altitudes. Journal of Geodesy, 2020, 94, 1.	1.6	23
23	Assessment and Validation of Three Ionospheric Models (IRIâ€2016, NeQuick2, and IGSâ€GIM) From 2002 to 2018. Space Weather, 2020, 18, e2019SW002422.	1.3	26
24	GPS + Galileo + BeiDou precise point positioning with triple-frequency ambiguity resolution. GF Solutions, 2020, 24, 1.	PS <sub>2.2</sub>	45
25	Hybrid constellation design using a genetic algorithm for a LEO-based navigation augmentation system. GPS Solutions, 2020, 24, 1.	2.2	36
26	Performance of GNSS Global Ionospheric Modeling Augmented by LEO Constellation. Earth and Space Science, 2020, 7, e2019EA000898.	1.1	13
27	Triple-frequency multi-GNSS reflectometry snow depth retrieval by using clustering and normalization algorithm to compensate terrain variation. GPS Solutions, 2020, 24, 1.	2.2	26
28	A method of improving ambiguity fixing rate for post-processing kinematic GNSS data. Satellite Navigation, 2020, 1, .	4.6	15
29	GPS inter-frequency clock bias estimation for both uncombined and ionospheric-free combined triple-frequency precise point positioning. Journal of Geodesy, 2019, 93, 473-487.	1.6	48
30	Estimation and analysis of differential code biases for BDS3/BDS2 using iGMAS and MGEX observations. Journal of Geodesy, 2019, 93, 419-435.	1.6	39
31	Kalman-filter-based undifferenced cycle slip estimation in real-time precise point positioning. GPS Solutions, 2019, 23, 1.	2.2	17
32	Attitude variometric approach using DGNSS/INS integration to detect deformation in railway track irregularity measuring. Journal of Geodesy, 2019, 93, 1571-1587.	1.6	14
33	Characterizing inter-frequency bias and signal quality for GLONASS satellites with triple-frequency transmissions. Advances in Space Research, 2019, 64, 1398-1414.	1.2	2
34	Performance evaluation of real-time global ionospheric maps provided by different IGS analysis centers. GPS Solutions, 2019, 23, 1.	2.2	44
35	A comparison of three widely used GPS triple-frequency precise point positioning models. GPS Solutions, 2019, 23, 1.	2.2	20
36	Mitigation of Unmodeled Error to Improve the Accuracy of Multi-GNSS PPP for Crustal Deformation Monitoring. Remote Sensing, 2019, 11, 2232.	1.8	15

#	Article	IF	CITATIONS
37	Multipath extraction and mitigation for high-rate multi-GNSS precise point positioning. Journal of Geodesy, 2019, 93, 2037-2051.	1.6	43
38	Differential Inter-System Biases Estimation and Initial Assessment of Instantaneous Tightly Combined RTK with BDS-3, GPS, and Galileo. Remote Sensing, 2019, 11, 1430.	1.8	23
39	Walker: Continuous and Precise Navigation by Fusing CNSS and MEMS in Smartphone Chipsets for Pedestrians. Remote Sensing, 2019, 11, 139.	1.8	20
40	Improving the Performance of Galileo Uncombined Precise Point Positioning Ambiguity Resolution Using Triple-Frequency Observations. Remote Sensing, 2019, 11, 341.	1.8	17
41	Improved PPP Ambiguity Resolution with the Assistance of Multiple LEO Constellations and Signals. Remote Sensing, 2019, 11, 408.	1.8	27
42	Estimating multi-frequency satellite phase biases of BeiDou using maximal decorrelated linear ambiguity combinations. GPS Solutions, 2019, 23, 1.	2.2	4
43	LEO constellation-augmented multi-GNSS for rapid PPP convergence. Journal of Geodesy, 2019, 93, 749-764.	1.6	93
44	Influencing Factors of GNSS Differential Inter-System Bias and Performance Assessment of Tightly Combined GPS, Galileo, and QZSS Relative Positioning for Short Baseline. Journal of Navigation, 2019, 72, 965-986.	1.0	15
45	Capturing coseismic displacement in real time with mixed single- and dual-frequency receivers: application to the 2018 Mw7.9 Alaska earthquake. GPS Solutions, 2019, 23, 1.	2.2	14
46	The improvement in integer ambiguity resolution with INS aiding for kinematic precise point positioning. Journal of Geodesy, 2019, 93, 993-1010.	1.6	41
47	Satellite availability and point positioning accuracy evaluation on a global scale for integration of GPS, GLONASS, BeiDou and Galileo. Advances in Space Research, 2019, 63, 2696-2710.	1.2	56
48	A comprehensive analysis of satellite-induced code bias for BDS-3 satellites and signals. Advances in Space Research, 2019, 63, 2822-2835.	1.2	31
49	Precise orbit determination for BDS3 experimental satellites using iGMAS and MGEX tracking networks. Journal of Geodesy, 2019, 93, 103-117.	1.6	42
50	Three-frequency BDS precise point positioning ambiguity resolution based on raw observables. Journal of Geodesy, 2018, 92, 1357-1369.	1.6	81
51	Quality assessment of GNSS observations from an Android N smartphone and positioning performance analysis using time-differenced filtering approach. GPS Solutions, 2018, 22, 1.	2.2	137
52	Multi-GNSS phase delay estimation and PPP ambiguity resolution: GPS, BDS, GLONASS, Galileo. Journal of Geodesy, 2018, 92, 579-608.	1.6	150
53	GPS inter-frequency clock bias modeling and prediction for real-time precise point positioning. GPS Solutions, 2018, 22, 1.	2.2	24
54	A New Method for GNSS Multipath Mitigation with an Adaptive Frequency Domain Filter. Sensors, 2018, 18, 2514.	2.1	8

#	Article	IF	CITATIONS
55	Assessment of precise orbit and clock products for Galileo, BeiDou, and QZSS from ICS Multi-GNSS Experiment (MGEX). GPS Solutions, 2017, 21, 279-290.	2.2	147
56	The contribution of Multi-GNSS Experiment (MGEX) to precise point positioning. Advances in Space Research, 2017, 59, 2714-2725.	1.2	59
57	Performance evaluation of single-frequency point positioning with GPS, GLONASS, BeiDou and Galileo. Survey Review, 2017, 49, 197-205.	0.7	45
58	Ambiguity resolved precise point positioning with GPS and BeiDou. Journal of Geodesy, 2017, 91, 25-40.	1.6	88
59	New optimal smoothing scheme for improving relative and absolute accuracy of tightly coupled GNSS/SINS integration. GPS Solutions, 2017, 21, 861-872.	2.2	34
60	Performance Evaluation of Single-frequency Precise Point Positioning with GPS, GLONASS, BeiDou and Galileo. Journal of Navigation, 2017, 70, 465-482.	1.0	49
61	Initial assessment of the COMPASS/BeiDou-3: new-generation navigation signals. Journal of Geodesy, 2017, 91, 1225-1240.	1.6	149
62	Influence of the GLONASS inter-frequency bias on differential code bias estimation and ionospheric modeling. GPS Solutions, 2017, 21, 1355-1367.	2.2	17
63	Evaluation of NTCM-BC and a proposed modification for single-frequency positioning. GPS Solutions, 2017, 21, 1535-1548.	2.2	8
64	Tightly Combined BeiDou B2 and Galileo E5b Signals for Precise Relative Positioning. Journal of Navigation, 2017, 70, 1253-1266.	1.0	10
65	Characteristics of inter-frequency clock bias for Block IIF satellites and its effect on triple-frequency GPS precise point positioning. GPS Solutions, 2017, 21, 811-822.	2.2	63
66	Considering Inter-Frequency Clock Bias for BDS Triple-Frequency Precise Point Positioning. Remote Sensing, 2017, 9, 734.	1.8	30
67	Instantaneous Real-Time Kinematic Decimeter-Level Positioning with BeiDou Triple-Frequency Signals over Medium Baselines. Sensors, 2016, 16, 1.	2.1	1,274
68	Global Ionospheric Modelling using Multi-GNSS: BeiDou, Galileo, GLONASS and GPS. Scientific Reports, 2016, 6, 33499.	1.6	73
69	Modeling and assessment of triple-frequency BDS precise point positioning. Journal of Geodesy, 2016, 90, 1223-1235.	1.6	108
70	Performance analysis of triple-frequency ambiguity resolution with BeiDou observations. GPS Solutions, 2016, 20, 269-281.	2.2	51
71	Benefits of the third frequency signal on cycle slip correction. GPS Solutions, 2016, 20, 451-460.	2.2	68
72	Generating GPS satellite fractional cycle bias for ambiguity-fixed precise point positioning. GPS Solutions, 2016, 20, 771-782.	2.2	64

#	Article	IF	CITATIONS
73	Receiver Time Misalignment Correction for GPS-based Attitude Determination. Journal of Navigation, 2015, 68, 646-664.	1.0	13
74	Detection of ionospheric disturbances driven by the 2014 Chile tsunami using GPS total electron content in New Zealand. Journal of Geophysical Research: Space Physics, 2015, 120, 7918-7925.	0.8	14
75	Observation of ionospheric disturbances induced by the 2011 Tohoku tsunami using far-field GPS data in Hawaii. Earth, Planets and Space, 2015, 67, .	0.9	11
76	Precise Point Positioning with Partial Ambiguity Fixing. Sensors, 2015, 15, 13627-13643.	2.1	52
77	A Novel Method for Precise Onboard Real-Time Orbit Determination with a Standalone CPS Receiver. Sensors, 2015, 15, 30403-30418.	2.1	35
78	Timing group delay and differential code bias corrections for BeiDou positioning. Journal of Geodesy, 2015, 89, 427-445.	1.6	100
79	BDS triple-frequency carrier-phase linear combination models and their characteristics. Science China Earth Sciences, 2015, 58, 896-905.	2.3	22
80	Performance enhancement for GPS positioning using constrained Kalman filtering. Measurement Science and Technology, 2015, 26, 085020.	1.4	5
81	High-precision coseismic displacement estimation with a single-frequency GPS receiver. Geophysical Journal International, 2015, 202, 612-623.	1.0	13
82	Precise positioning with current multi-constellation Global Navigation Satellite Systems: GPS, GLONASS, Galileo and BeiDou. Scientific Reports, 2015, 5, 8328.	1.6	264
83	Modeling and Performance Analysis of GPS/GLONASS/BDS Precise Point Positioning. Lecture Notes in Electrical Engineering, 2014, , 251-263.	0.3	4
84	Improved precise point positioning in the presence of ionospheric scintillation. GPS Solutions, 2014, 18, 51-60.	2.2	54
85	Real-time clock jump compensation for precise point positioning. GPS Solutions, 2014, 18, 41-50.	2.2	32
86	Integrating GPS and GLONASS to accelerate convergence and initialization times of precise point positioning. GPS Solutions, 2014, 18, 461-471.	2.2	147
87	Predicting atmospheric delays for rapid ambiguity resolution in precise point positioning. Advances in Space Research, 2014, 54, 840-850.	1.2	19
88	Daily Global Plasmaspheric Maps Derived From COSMIC GPS Observations. IEEE Transactions on Geoscience and Remote Sensing, 2014, 52, 6040-6046.	2.7	16
89	Adaptive robust Kalman filtering for precise point positioning. Measurement Science and Technology, 2014, 25, 105011.	1.4	41
90	Global multiple tropopause features derived from COSMIC radio occultation data during 2007 to 2012. Journal of Geophysical Research D: Atmospheres, 2014, 119, 8515-8534.	1.2	7

#	Article	IF	CITATIONS
91	A Multi-Step Multi-Order Numerical Difference Method for Traveling Ionospheric Disturbances Detection. Lecture Notes in Electrical Engineering, 2014, , 331-340.	0.3	3
92	Integration of GNSS and Seismic Data for Earthquake Early Warning: A Case Study on the 2011 Mw 9.0 Tohoku-Oki Earthquake. Lecture Notes in Electrical Engineering, 2014, , 437-450.	0.3	2
93	Ambiguity resolution in precise point positioning with hourly data for global single receiver. Advances in Space Research, 2013, 51, 153-161.	1.2	35
94	Assessment of correct fixing rate for precise point positioning ambiguity resolution on a global scale. Journal of Geodesy, 2013, 87, 579-589.	1.6	35
95	Influence of clock jump on the velocity and acceleration estimation with a single GPS receiver based on carrier-phase-derived Doppler. GPS Solutions, 2013, 17, 549-559.	2.2	13
96	Realâ€ŧime highâ€ŧate coâ€seismic displacement from ambiguityâ€fixed precise point positioning: Application to earthquake early warning. Geophysical Research Letters, 2013, 40, 295-300.	1.5	87
97	Application of Collocated GPS and Seismic Sensors to Earthquake Monitoring and Early Warning. Sensors, 2013, 13, 14261-14276.	2.1	10
98	Improving the Estimation of Uncalibrated Fractional Phase Offsets for PPP Ambiguity Resolution. Journal of Navigation, 2012, 65, 513-529.	1.0	79
99	A novel Stop&Go GPS precise point positioning (PPP) method and its application in geophysical exploration and prospecting. Survey Review, 2012, 44, 251-255.	0.7	3
100	Satellite clock estimation at 1ÂHz for realtime kinematic PPP applications. GPS Solutions, 2011, 15, 315-324.	2.2	105
101	Regional reference network augmented precise point positioning for instantaneous ambiguity resolution. Journal of Geodesy, 2011, 85, 151-158.	1.6	200
102	Serverâ€Based Realâ€Time Precise Point Positioning and Its Application. Chinese Journal of Geophysics, 2010, 53, 372-379.	0.2	6
103	Retrieval of Airborne Lidar Misalignments Based on the Stepwise Geometric Method. Survey Review, 2010, 42, 176-192.	0.7	1
104	Impact of sampling rate of IGS satellite clock on precise point positioning. Geo-Spatial Information Science, 2010, 13, 150-156.	2.4	13
105	Assessment of long-range kinematic GPS positioning errors by comparison with airborne laser altimetry and satellite altimetry. Journal of Geodesy, 2007, 81, 201-211.	1.6	19
106	Surface Ice Flow Velocity and Tide Retrieval of the Amery Ice Shelf using Precise Point Positioning. Journal of Geodesy, 2006, 80, 171-176.	1.6	54